Available online at www.sciencedirect.com

ScienceDirect

Energy Procedia 63 (2014) 940 – 950

Energy Procedia

GHGT-12

Modeling of oxidative MEA degradation

Diego D. D. Pinto[a], Thea W. Brodtkorb[a], Solrun J. Vevelstad[b], Hanna Knuutila[a], Hallvard F. Svendsen[a,*]

[a]*Department of Chemical Engineering, Norwegian University of Science and Technology, N-7491 Trondheim, Norway*
[b]*SINTEF Materials and Chemistry*

Abstract

Considerable amount of work had been recently done researching the degradation of solvents for CO_2 post combustion capture, especially for the benchmark solvent MEA. The degradation of the solvent can cause plant corrosion and losses in the process performance since the solvent might loses its capacity to absorb CO_2. Thus, a better understanding of this phenomena is important for the overall process performance. Oxidative degradation is likely to occur at absorber conditions due to the presence of oxygen in the flue gas. Differently from the thermal degradation, the oxidative degradation is not well understood. This work presents a preliminary attempt to rigorously model the degradation of solvents for CO_2 capture. Experimental data available in the literature were used to regress some of the model parameters. Several assumptions had to be made due to the lack of knowledge. The model, however, does a reasonable job of representing the dynamic trends of the oxidative degradation in the MEA system. This model is still under further development and new components, experiments and reactions are being implemented in the model.

Peer-review under responsibility of the Organizing Committee of GHGT-12

Keywords: Oxidative degradation; MEA; CO_2 capture; amine scrubbing; post-combustion

1. Introduction

Chemical absorption processes with amines are the most mature, well-understand and used technology for post combustion CO_2 capture [1]. Despite the new trend for developing new solvents, or solvent blends for CO_2 capture,

* Corresponding author. Tel.: +47 7359 4100; fax: +47 7359 4080.
E-mail address: hallvard.svendsen@chemeng.ntnu.no

Peer-review under responsibility of the Organizing Committee of GHGT-12
doi:10.1016/j.egypro.2014.11.103

monoethanolamine (MEA) is still the benchmark solvent. Much data on the physical and thermodynamic properties for pure MEA, binary MEA-H_2O and ternary MEA-H_2O-CO_2 are available in the literature.

Nomenclature

a	Mass transfer area per unit volume of continuous phase (m^2/m^3)
C	Molar concentration ($kmol/m^3$)
G	molar gas flow rate (kmol/day)
H	Henry's constant ($bar.m^3/kmol$)
K_G	Overall gas-phase mass transfer coefficient
P	Pressure (bar)
R	Universal gas constant ($bar.m^3/(K.kmol)$)
T	Temperature (K)
V_L	Volume of the liquid phase (m^3)
y	Mole fraction of a component in the gas phase
subscripts	
in	Reactor inlet condition
out	Reactor outlet condition
i, j	component counter

Due to the restrictions on solvent emissions, degradation studies concerning alkanolamines in post combustion process have increased considerably. In a post-combustion CO_2 capture process, degradation compounds can be formed by three routes: (i) Oxidative degradation, most likely to occur in the absorber and heat exchanger; (ii) Thermal degradation with CO_2, likely to occur in the stripper and reboiler; and (iii) Thermal degradation, not so common due to the elevated temperatures required [2].

Thermal degradation appears to be well understood while a better understanding is needed for oxidative degradation [3]. Also, the oxidative and thermal degradation are coupled, implying that the oxidative degradation in the absorber will influence the thermal processes in the other process parts. Lepaumier, et al. [4], da Silva, et al. [3] and Vevelstad, et al. [5] used an open batch reactor to study the oxidative degradation of MEA. In this work, a model for the open batch reactor used by those authors is proposed. The resulting model is able to predict the amine loss and most of the degradation compounds quantified by Vevelstad, et al. [5].

2. The open batch reactor

In the open batch reactor experiment a 30 % (weight) aqueous MEA solution was pre-loaded (α = 0.4 mol CO_2/mol MEA) and inserted into the reactor. The liquid phase in the reactor was agitated by a magnetic stirrer and the temperature controlled by and external water bath.

The gas phase was recirculated and a small amount of gas, a mixture of 98% oxygen/nitrogen and 2% CO_2 was injected throughout the experiment. The entering gas was saturated in a water tank prior to injection at the bottom of the reactor through a sinter providing very small bubbles. The gas phase leaves at the top of the reactor and most of it was recycled to the reactor using a gas pump. At the top of the reactor a cooler was used to condense the volatile compounds (e.g., water, amine, ammonia). After the cooler, the gas was sent to an acidic wash to remove the basic compounds not condensed in the cooler, and released to the atmosphere. Liquid samples were taken periodically from the reactor and the acidic wash bottle. The concentration of O_2 and the temperature of the reactor were varied from 6 to 98% and from 55 to 75ºC, respectively. A more detailed description on the operation and analytical procedures can be found in Vevelstad, et al. [5].

2.1. Proposed reactions

The samples were analyzed using different analytical techniques as Liquid Chromatography- Mass Spectrometry (LC-MS) and Ion Chromatography (IC). For the LC-MS an LC-MS-MS 6460 Triple Quadropole Mass Spectrometer

coupled with a 1290 Infinity LC Chromatograph and an Infinity Autosampler 1200 Series G4226A from the supplier Agilent Technologies were used. The eluent, the analytical column and ion source varied depending on the compound. Details are described by da Silva, et al. [3] and Vevelstad, et al. [5]. MEA, formaldehyde, HEF, HEI, BHEOX, HEGly and ammonia were analyzed on LC-MS and internal standards were used for MEA, formaldehyde and ammonia. The acids; oxalic and formic acid were analyzed on anion IC using an ICS-5000 system from Dionex. A more detailed description of the system is given by Vevelstad, et al. [5]. Over 20 compounds (including MEA) were quantified, but only 8 of them were initially chosen for the modeling. The formation of the 8 compounds are described by 8 suggested reactions. Table 1 shows the degradation compounds considered in the modeling.

Table 1. Oxidative degradation compounds considered in the modeling.

Name	Abbreviation	CAS	Quantified
Formaldehyde	CH2O	50-00-0	No
Formic acid	CH2O2	64-19-7	Yes
Glyoxal	C2H2O2	107-22-2	No
Oxalic acid	C2H2O4	144-62-7	Yes
N-(2-hydroxyethyl) formamide	HEF	693-06-1	Yes
N-(2-hydroxyethyl) imidazole	HEI	1615-14-1	Yes
N,N'-bis(2- hydroxyethyl) oxalamide	BHEOX	1871-89-2	Yes
N-(2- hydroxyethyl) glycine	HEGly	5835-28-9	Yes
Ammonia	NH3	7664-41-7	Yes

The following reactions were used in the model to describe the degradation pathway.

$$MEA + 3H_2O \rightarrow 2CH_2O + NH_3 + 2H_3O^+ + 2e^- \quad (1)$$

$$CH_2O + {}^{1}\!/\!_{2}\, O_2 \rightarrow CH_2O_2 \quad (2)$$

$$MEA + CH_2O_2 \rightleftarrows HEF + H_2O \quad (3)$$

$$MEA + O_2 \rightarrow C_2H_2O_2 + H_2O + NH_3 \quad (4)$$

$$MEA + CH_2O + C_2H_2O_2 + NH_3 \rightleftarrows HEI + 3H_2O \quad (5)$$

$$C_2H_2O_2 + O_2 \rightarrow C_2H_2O_4 \quad (6)$$

$$2MEA + C_2H_2O_4 \rightleftarrows BHEOX + 2H_2O \quad (7)$$

$$2MEA + \frac{1}{2} O_2 + 2H_2O \rightleftarrows HEGly + NH3 + 2H_3O^+ + 2e^- \quad (8)$$

Reaction 1 shows the formation of formaldehyde. This reaction is believed to follow a hydrogen abstraction mechanism which requires a radical initiator. Although this is not shown explicitly in the reaction, oxygen will create the radical needed for the reaction.

The formation of formic acid is shown in reaction 2. This reaction is a simple oxidation of formaldehyde since aldehydes are known to be quickly oxidized to acids even with air [6].

Glyoxal was proposed to form in a two-step reaction. First, MEA reduces to acetaldehyde and ammonia. Acetaldehyde is further reacted with oxygen to form glyoxal and water. Assuming a pseudo steady state for the acetaldehyde, the reactions can be combined and the final reaction is shown in reaction 3.

Oxalic acid formation has been proposed by several authors and different mechanisms can be found. Buxton, et al. [7] describes the oxidation of glyoxal via glyoxylic acid to oxalic acid, initiated by •OH-radicals, in presence of oxygen. Although there is no evidence to support any of the routes, this was the one chosen to represent the formation of oxalic acid and is shown in reaction 4.

Lepaumier, et al. [4] and Supap, et al. [8] have suggested a mechanism for the HEF formation. This reaction is implemented in the model and is given in reaction 5. HEI formation (reaction 6) has been documented by Arduengo, et al. [9], Ben [10] and Katsuura and Washio [11] and was used in the present model.

Reaction 7 shows the BHEOX formation. This reaction is reported in Lepaumier, et al. [4]. Reaction 8 represents the formation of HEGly. The detailed reaction pathway to HEGly is rather uncertain. However, there is a mechanism suggested for the formation of HEGly [12], but more tests are needed for its verification.

3. Degradation model

The open batch reactor is classified as a semi flow batch reactor (SFBR) since only the gas flows through the reactor [13]. The liquid phase composition is considered to vary over time but is spatially invariant, i.e. well mixed. By applying a general mass balance it is possible to model the gas and liquid phases according to Eqs. 9 to 11.

$$G_{in} y_{0_j} - G_{out} y_j - K_{G,j} a V_L P \left(y_j - C_j \frac{H_j}{P} \right) = 0 \quad (9)$$

$$K_{G,j} a P \left(y_j - C_j \frac{H_j}{P} \right) - R_{x,j} = \frac{dC_j}{dt} \quad (10)$$

$$K_{G,j} a P \left(\frac{G_{in} y_{0_j} + K_{G,j} a V_L C_j H_j}{G_{out} + K_{G,j} a V_L P} - C_j \frac{H_j}{P} \right) - R_{x,j} = \frac{dC_j}{dt} \quad (11)$$

Because of the low gas phase retention time, the gas phase equation (Eq. 9) is based on a steady state condition, but is coupled to the time dependency in the liquid phase composition. The mol fraction in the gas phase can be isolated and inserted in the liquid phase equation (Eq. 10) and the resulting differential equation (Eq. 11) can be solved for the liquid phase composition.

The reaction rates are calculated according to a general form given in Eq. 12 where the reaction rate coefficients $\left(k_i \text{ and } k_{-i}\right)$ and the reaction orders $\left(r_{i,j} \text{ and } r_{-i,j}\right)$ are fitted to the experimental data.

$$R_{x,i} = k_i \prod_{j=1}^{N} C_j^{r_{i,j}} - k_{-i} \prod_{j=1}^{N} C_j^{r_{-i,j}} \quad (12)$$

Additionally, the reaction rate coefficients are assumed to have an Arrhenius equation form to account for the temperature dependency, as shown in Eq. 13.

$$k_i = A_i \exp\left(\frac{-E_{Ai}}{RT}\right) \quad (13)$$

3.1. Overall mass transfer coefficient

Eq. 14 defines the overall mass transfer coefficient. In this work, the gas side mass transfer coefficient was fixed at 0.01 m/s for all temperatures and concentrations. However, the liquid side mass transfer coefficient will have a temperature dependency to account for the calculations at different temperatures. The correlation taken from Cussler [14] (p. 226 table 8.3-2) for pure gas bubbles in an unstirred liquid (Eq. 15) can be applied in the model since the magnetic stirrer in the experiment was not strong enough to be considered a stirred tank.

Han, et al. [15] provide experimental values for density for loaded solutions of 30% wt. of MEA. However, there is no data for 0.4 loading. Therefore, the density for loaded MEA (30% wt.) at 0.4 loading is generated interpolating the experimental data for loading at 0.32 and 0.44.

$$\frac{1}{K_G} = \frac{H}{k_L} + \frac{1}{k_G} \quad (14)$$

$$k_L = \frac{D}{d} 0.31 \left(\frac{d^3 g \, \Delta\rho / \rho}{\nu^2} \right)^{1/3} \left(\frac{\nu}{D} \right)^{1/3} \quad (15)$$

Table 2. Parameters for the Wilke-Chang correlation (equation **Error! Reference source not found.**).

Parameter		Value
ϕ	Association parameter	2.6
M_B	Molecular weight of the solvent [kg/mol]	22.3987
T	Temperature [K]	-
μ_B	Dynamic viscosity [kg/m.s]	-
V_A	Molecular volume of the solute [kmol/m^3]	
	O2	0.0256
	MEA	0.0785
	Formaldehyde	0.0294
	NH3	0.0258
	H2O	0.0188

The diffusivity of MEA in the solution was estimated by the Wilke-Chang correlation (Eq. 16). This is a semi-empirical model for solutes with small solute volumes. The parameters for the diffusivity correlation are given in Table 2. The temperature dependency in Eq. 15 is given by the viscosity, densities and diffusion coefficients.

$$D_{AB} = 1.173 \cdot 10^{-16} \left(\phi M_B\right)^{0.5} \frac{T}{\mu_B V_A^{0.6}} \quad (16)$$

3.2. Henry's constant

The solubility of the compounds in a solvent can be determined by the Henry's constant. The Henry's constant is defined as the partial pressure of a component above a solution divided by its solution concentration. Rooney and Daniels [16] correlated the Henry's constant for oxygen in a 20 mass% MEA solution (Eq. 17). The correlation is given in pressure units (atm, mol fraction basis), and is easily converted to concentration basis by using the density of the solution. This correlation is used in this work. The oxygen solubility in unloaded amine solutions are expected to be higher than in loaded solutions [17]. By using the correlation in Eq. 17 it is thus assumed that more O_2 is dissolved in the liquid phase than what really is, but no model giving oxygen solubility as function of temperature, amine concentration and CO_2 loading is available.

$$\ln\left(H\right) = 3.71814 + \frac{5596.17}{T} - \frac{1049668}{T^2} \quad (17)$$

The volatility of MEA is calculated by calculating the partial pressure of MEA according to Eq. 18. The activity coefficient was calculated through an NRTL model and the MEA saturation pressure was calculated with an Antoine model. The parameters for both the NRTL and Antoine models are taken from Kim, et al. [18].

$$P_{MEA} = P_{MEA}^{sat} x_{MEA} \gamma_{MEA} \quad (18)$$

Allou, et al. [19] give a correlation for calculating the Henry's constant (kmol.m^{-3}.atm^{-1}) of formaldehyde in pure water from 273 to 293 K. This correlation, given in Eq. 19, is used in this work.

$$\ln\left(H_{Form}\right) = \frac{6423}{T} - 13.4 \quad (19)$$

Bieling, et al. [20] present a Henry's constant model for the solubility of NH_3 in water used in this work (Eq.20). The Henry's constant is given in (MPa.kg.mol^{-1}) and the temperature in K.

$$\ln\left(H_{NH_3}\right) = 3.932 - \frac{1879}{T} - \frac{3.551 \cdot 10^5}{T^2} \quad (20)$$

For the other components no data or correlations were available in the literature. Therefore, models based on computational chemistry, according to Eq. 21, were developed and implemented in the overall model. H^{dim} is the dimensionless Henry's constant calculated through computational chemistry.

$$H = RT \cdot H^{\dim} \qquad (21)$$

4. Results

The results for the optimization of the parameters are shown from Figures 1 to 7. The experiments with 21% O_2 concentration at 55, 65 and 75ºC were used to fit the model parameters while the experiments performed at 55ºC with 50 and 98% O_2 concentration were used to validate the model. As shown in Figure 1, MEA degrades more as more oxygen is present in the gas stream. The temperatures also affect the degradation rates. The higher the temperature, the higher the MEA degradation. The model is able to well represent the MEA loss.

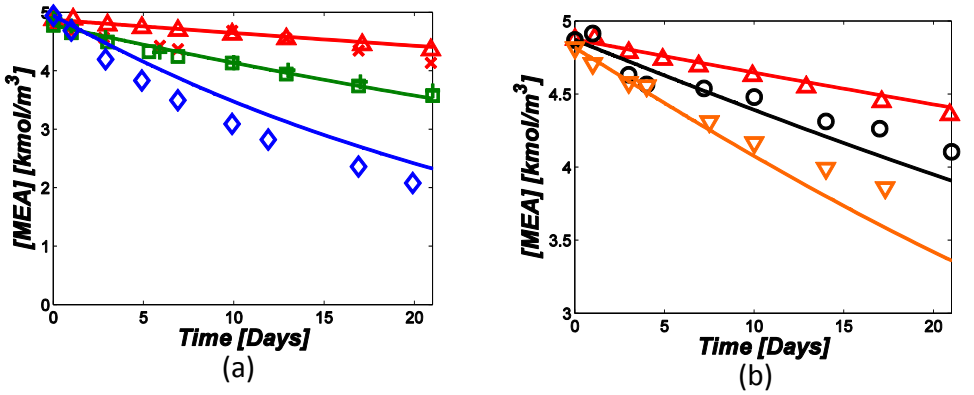

Figure 1. MEA concentration profiles at: (a) 21% [O_2] and (Δ,x) at 55ºC, (□,+) at 65ºC and (◊) at 75ºC; and (b) at 55ºC and (Δ) 21% [O_2], (○) 50% [O_2] and (▽) 98% [O_2]

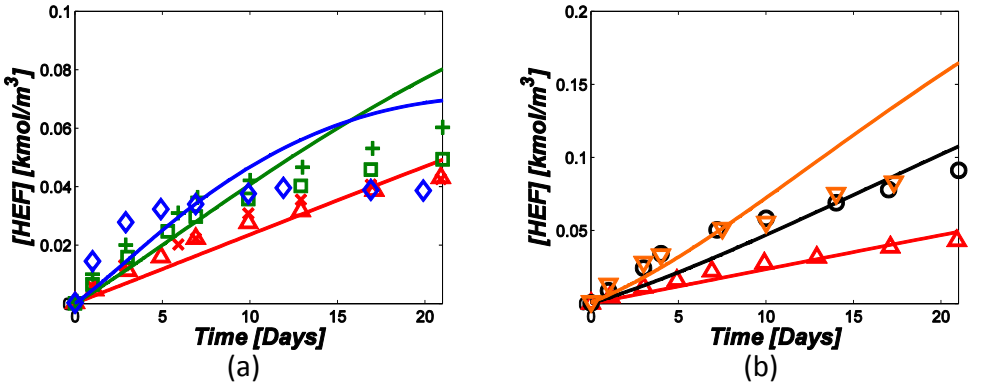

Figure 2. HEF concentration profiles at: (a) 21% [O_2] and (Δ,x) at 55ºC, (□,+) at 65ºC and (◊) at 75ºC; and (b) at 55ºC and (Δ) 21% [O_2], (○) 50% [O_2] and (▽) 98% [O_2]

The formation of HEF, shown in Figure 2, is well represented by the model at 55ºC and 21% oxygen concentration. At high temperature (75ºC) the concentration of HEF seems to stabilize. Increasing the oxygen concentration above 50% seems not to influence in the concentration of HEF at 55ºC.

The model represents the data well at 21% oxygen, but fails to represent the formation of HEI at high oxygen concentration. From Figure 3, however, it is clearly seen that the parallel experiments done at 21% oxygen show a

large deviation between the experimental points. The deviation between the parallels might be explained by improvements in the analytical methods used to quantify the degradation compounds.

Oxalic acid is well represented by the model, except when the gas phase has 98% oxygen concentration. The parallel experiments agree quite well with each other as shown in Figure 4. Figure 5 shows the BHEOX concentrations. The model is able to well represent the formation of BHEOX given the scatter in the data. At 21% oxygen and at 75ºC the experiment suggests that the concentration of BHEOX starts to level off and decrease after three days. This behavior is captured by the model.

As presented in Figure 6, HEGly seems to be indifferent to the concentration of oxygen in the gas stream whereas the model predicts that the concentration of HEGly is directly proportional to the oxygen content in the gas phase. As for the BHEOX, the HEGly concentration at 75ºC and 21% starts to decrease after 6-7 days. The model is able to capture this trend.

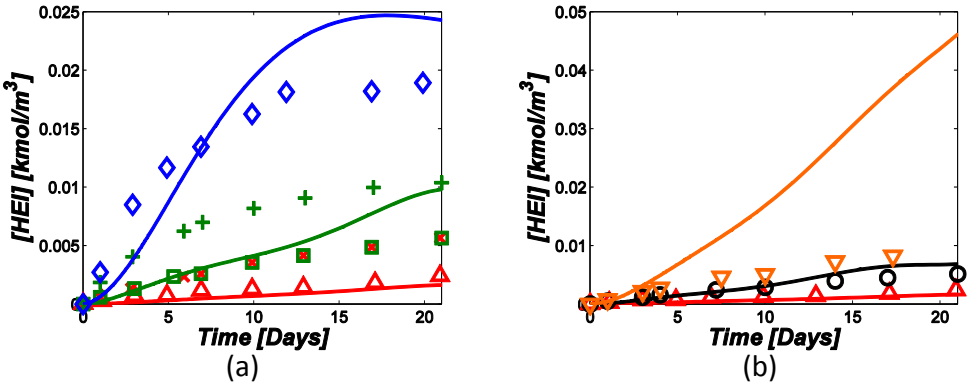

Figure 3. HEI concentration profile at: (a) 21% [O_2] and (Δ,x) at 55ºC, (□,+) at 65ºC and (◊) at 75ºC; and (b) at 55ºC and (Δ) 21% [O_2], (○) 50% [O_2] and (▽) 98% [O_2]

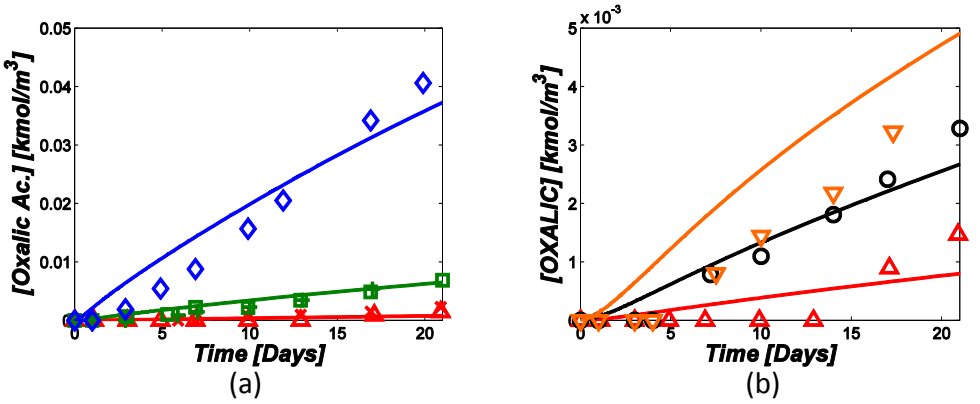

Figure 4. Oxalic acid concentration profile at: (a) 21% [O_2] and (Δ,x) at 55ºC, (□,+) at 65ºC and (◊) at 75ºC; and (b) at 55ºC and (Δ) 21% [O_2], (○) 50% [O_2] and (▽) 98% [O_2]

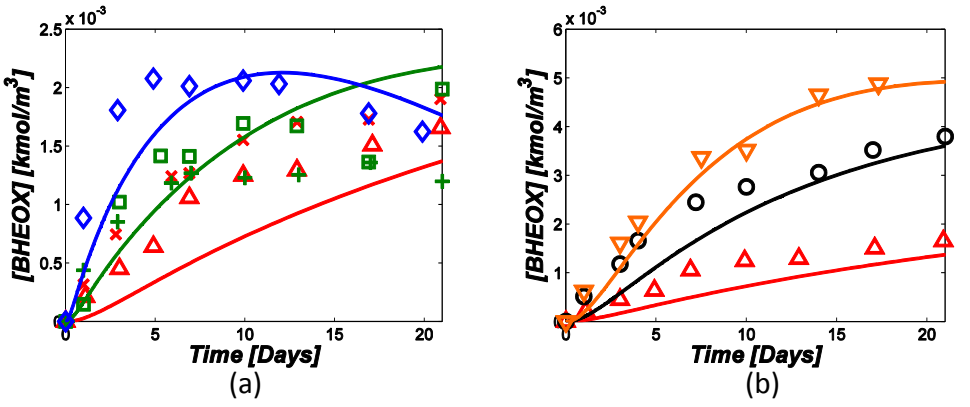

Figure 5. BHEOX concentration profile at: (a) 21% [O_2] and (Δ,x) at 55ºC, (□,+) at 65ºC and (◊) at 75ºC; and (b) at 55ºC and (Δ) 21% [O_2], (○) 50% [O_2] and (▽) 98% [O_2]

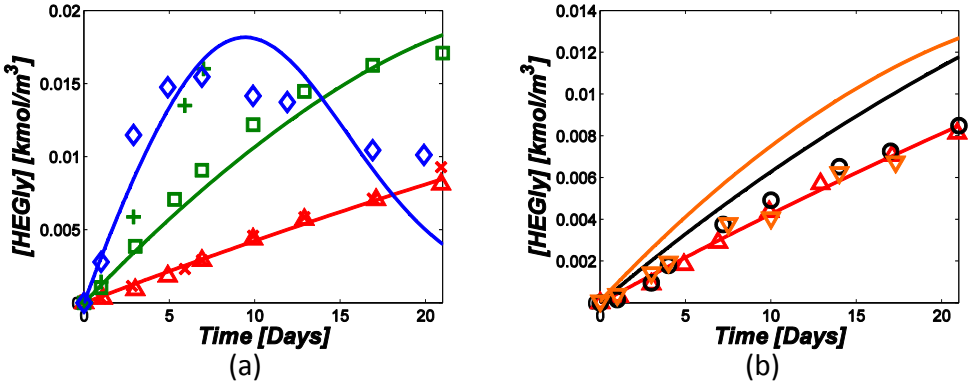

Figure 6. HEGly concentration profile at: (a) 21% [O_2] and (Δ,x) at 55ºC, (□,+) at 65ºC and (◊) at 75ºC; and (b) at 55ºC and (Δ) 21% [O_2], (○) 50% [O_2] and (▽) 98% [O_2]

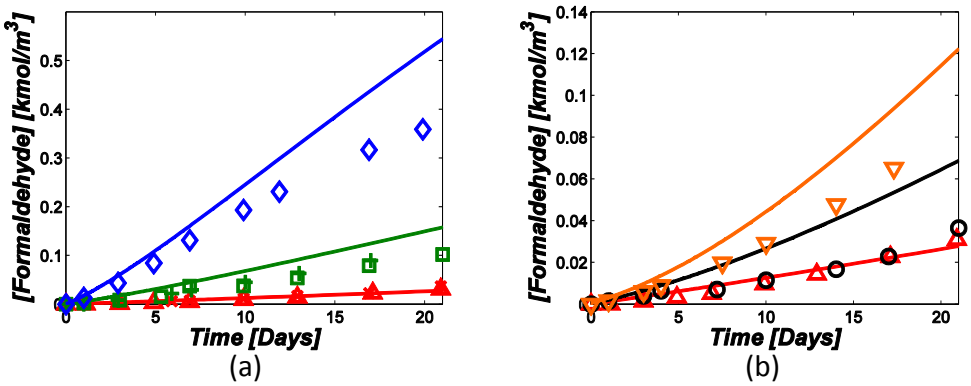

Figure 7. Formaldehyde concentration profile at: (a) 21% [O_2] and (Δ,x) at 55ºC, (□,+) at 65ºC and (◊) at 75ºC; and (b) at 55ºC and (Δ) 21% [O_2], (○) 50% [O_2] and (▽) 98% [O_2]

The concentration of formaldehyde is presented in Figure 7. The rate of formation of formaldehyde seems to be unaffected by the gas stream oxygen concentrations up to 50%. This trend is not captured by the model which

predicts increasing concentrations of formaldehyde in the liquid phase as the concentration of oxygen is increased in the gas phase. However, in this case the experimental points may be in uncertain.

5. Conclusions

A model is developed for prediction the rate of degradation of MEA and the rate of formation of 6 degradation products. The model is found to be able to represent the general trends of the oxidative degradation of the MEA system as it is able to both predict the loss of MEA at the absorber conditions and also the build-up of degradation products.

Both the model and the experiments carry uncertainties. On the experimental side, the analytical methods are in constant development and this might explain differences seen in parallel runs performed a year apart. The number of degradation compounds analyzed for, as mentioned before, is higher than what is presented in this work and the reactions chosen to represent the system might still need refinement for modeling the oxidative degradation. The physical property data, in particular gas solubilities, are other sources of uncertainties in the model. In some cases, due to the lack of data, assumptions had to be made in order to build the model. There is still a lot of work remaining before a model can be implemented with a high degree of confidence. The model presented is, however, a good first attempt to rigorous modeling of the degradation of a solvent for CO_2 capture. The model is under further development and new components, experiments and reactions are being implemented in the model.

Acknowledgements

Financial support from the European FP7 iCap project (Grant Agreement n° 241391), from the European FP7 OCTAVIUS project (Grant Agreement n° 295645) and from NTNU Strategic Funds is gratefully acknowledged.

References

[1] G.T. Rochelle, Amine Scrubbing for CO_2 Capture, Science, 325 (2009) 1652-1654.
[2] S. Chi, G.T. Rochelle, Oxidative Degradation of Monoethanolamine, Industrial & Engineering Chemistry Research, 41 (2002) 4178-4186.
[3] E.F. da Silva, H. Lepaumier, A. Grimstvedt, S.J. Vevelstad, A. Einbu, K. Vernstad, H.F. Svendsen, K. Zahlsen, Understanding 2-Ethanolamine Degradation in Postcombustion CO_2 Capture, Industrial & Engineering Chemistry Research, 51 (2012) 13329-13338.
[4] H. Lepaumier, E.F. da Silva, A. Einbu, A. Grimstvedt, J.N. Knudsen, K. Zahlsen, H.F. Svendsen, Comparison of MEA degradation in pilot-scale with lab-scale experiments, Energy Procedia, 4 (2011) 1652-1659.
[5] S.J. Vevelstad, A. Grimstvedt, J. Elnan, E.F. da Silva, H.F. Svendsen, Oxidative degradation of 2-ethanolamine: The effect of oxygen concentration and temperature on product formation, International Journal of Greenhouse Gas Control, 18 (2013) 88-100.
[6] C. Gouedard, D. Picq, F. Launay, P.L. Carrette, Amine degradation in CO_2 capture. I. A review, International Journal of Greenhouse Gas Control, 10 (2012) 244-270.
[7] G.V. Buxton, T.N. Malone, G. Arthur Salmon, Oxidation of glyoxal initiated by OH in oxygenated aqueous solution, Journal of the Chemical Society, Faraday Transactions, 93 (1997) 2889-2891.
[8] T. Supap, R. Idem, P. Tontiwachwuthikul, Mechanism of formation of heat stable salts (HSSs) and their roles in further degradation of monoethanolamine during CO_2 capture from flue gas streams, Energy Procedia, 4 (2011) 591-598.
[9] A.J. Arduengo, F.P.G. Jr., P.K. Taverkere, H.E. Simmons, Process for manufacture of imidazoles, in, 2001.
[10] D.S.P. Ben, Process for the preparation of -1-(2-hydroxyethyl) imidazole, in, 2005, pp. 6pp.
[11] A. Katsuura, N. Washio, Preparation of imidazoles from imines and iminoacetaldehydes, in, 2005, pp. 6 pp.
[12] S.J. Vevelstad, A. Grimstvedt, H. Knuutila, E.F. da Silva, H.F. Svendsen, Influence of experimental setup on amine degradation, International Journal of Greenhouse Gas Control, 28 (2014) 156-167.

[13] R.W. Schaftlein, T.W.F. Russell, TWO-PHASE REACTOR DESIGN. TANK-TYPE REACTORS, Industrial & Engineering Chemistry, 60 (1968) 12-27.
[14] E.L. Cussler, Diffusion : Mass Transfer in Fluid Systems (Cambridge Series in Chemical Engineering), Cambridge University Press, 1997.
[15] J. Han, J. Jin, D.A. Eimer, M.C. Melaaen, Density of Water (1) + Monoethanolamine (2) + CO2 (3) from (298.15 to 413.15) K and Surface Tension of Water (1) + Monoethanolamine (2) from (303.15 to 333.15) K, Journal of Chemical & Engineering Data, 57 (2012) 1095-1103.
[16] P.C. Rooney, D.D. Daniels, Oxygen solubility in various alkanolamine/water mixtures, Petroleum Technology Quarterly, (1998) 97 - 101.
[17] M.H. Wang, A. Ledoux, L. Estel, Oxygen Solubility Measurements in a MEA/H_2O/CO_2 Mixture, Journal of Chemical & Engineering Data, 58 (2013) 1117-1121.
[18] I. Kim, H.F. Svendsen, E. Børresen, Ebulliometric Determination of Vapor−Liquid Equilibria for Pure Water, Monoethanolamine, N-Methyldiethanolamine, 3-(Methylamino)-propylamine, and Their Binary and Ternary Solutions, Journal of Chemical & Engineering Data, 53 (2008) 2521-2531.
[19] L. Allou, L. El Maimouni, S. Le Calvé, Henry's law constant measurements for formaldehyde and benzaldehyde as a function of temperature and water composition, Atmospheric Environment, 45 (2011) 2991-2998.
[20] V. Bieling, B. Rumpf, F. Strepp, G. Maurer, An evolutionary optimization method for modeling the solubility of ammonia and carbon dioxide in aqueous solutions, Fluid Phase Equilibria, 53 (1989) 251-259.